

Integrative Machine Learning Analysis of Programmed Cell Death Pathways Identifies Novel Diagnostic Biomarkers for Atrial Fibrillation

Hongbo Peng*, Zhenwei Xia*, Yangyang Zhao, Di Xie 

Department of Cardiology, Central Hospital of Dalian University of Technology, Dalian, Liaoning, People's Republic of China

*These authors contributed equally to this work

Correspondence: Di Xie, Department of Cardiology, Central Hospital of Dalian University of Technology, 826 Xinan Road, Dalian, Liaoning, People's Republic of China, Email xd_carrot@163.com

Purpose: Atrial fibrillation (AF) is a leading cause of stroke, heart failure, and mortality, yet the molecular mechanisms remain incompletely defined.

Patients and Methods: We integrated bulk transcriptomes from GEO with weighted gene co-expression network analysis, consensus clustering, and a 12-algorithm machine-learning pipeline (66 model combinations) to map programmed cell death (PCD) pathways and pinpoint diagnostic genes. Immune infiltration was profiled by CIBERSORT, xCell, and ssGSEA. Hub-gene expression was validated in an HL-1 atrial pacing model and in peripheral blood mononuclear cells (PBMCs) from patients with persistent AF.

Results: Four hub genes—SGPL1, NPC2, PTGDS, and RCAN1—were identified and incorporated into a nomogram and a PCD-based risk score (PCDscore). The nomogram showed robust discrimination in the training cohort and two independent validation datasets. Patients with a high PCDscore exhibited markedly increased immune-cell infiltration and dysregulated immune modulators, with macrophages consistently enriched across algorithms. qRT-PCR confirmed up-regulation of SGPL1, NPC2, and RCAN1 and down-regulation of PTGDS in AF cell models; NPC2 and SGPL1 were further elevated in PBMCs from AF patients.

Conclusion: Our integrative framework reveals PCD-linked remodeling in AF and nominates SGPL1, NPC2, PTGDS, and RCAN1 as candidate diagnostic biomarkers, providing a PCD-based nomogram and risk score that may inform patient stratification and hypothesis-generating targeted interventions.

Keywords: cardiac arrhythmias, immune remodeling, macrophage infiltration, molecular subtyping, apoptosis, diagnostic nomogram

Introduction

Atrial fibrillation (AF) is the most prevalent sustained cardiac arrhythmia worldwide, currently affecting more than 33 million individuals and posing significant public health burdens due to its growing incidence and association with substantial morbidity and mortality.^{1,2} Clinically, AF is closely linked to increased risks of ischemic stroke, heart failure, and sudden cardiac death, imposing considerable socio-economic challenges on healthcare systems globally.³ At the molecular level, AF results from intricate electrophysiological and pathological processes, including electrical and structural remodeling, impaired calcium handling, and atrial fibrosis.^{1,4} Despite significant advancements in pharmacological therapies and catheter ablation techniques, the effectiveness of these treatments remains limited, particularly for persistent AF, which is characterized by high recurrence rates, suboptimal outcomes, and resistance to halting disease progression.^{5–7} The suboptimal efficacy and lack of personalization in existing therapeutic strategies reflect a critical gap in our comprehensive understanding of the underlying molecular mechanisms driving AF development and progression.

Programmed cell death (PCD), a highly regulated cellular process involving the selective elimination of damaged or unnecessary cells, has recently gained attention for its complex role in cardiovascular diseases. At present, multiple subtypes of PCD have been extensively characterized, including apoptosis, necroptosis, pyroptosis, ferroptosis, autophagy-dependent cell death, lysosome-dependent cell death, and cuproptosis.^{8,9} Growing evidence indicates that dysregulated PCD contributes significantly to pathological processes such as myocardial remodeling, chronic inflammation, endothelial dysfunction, and cardiomyocyte loss, thus playing critical roles in myocardial infarction, heart failure, and atherosclerosis.^{10–13}

However, the specific roles of PCD in the pathogenesis of AF remain incompletely understood and understudied. Recent evidence has suggested that certain types of PCD, including apoptosis and ferroptosis, may facilitate atrial remodeling processes, characterized by progressive fibrosis, impaired calcium handling, and increased oxidative stress, all of which potentially contribute to the initiation and maintenance of AF.^{14–16} Nonetheless, existing studies have largely examined these PCD subtypes in isolation, without comprehensive, integrative analyses across multiple datasets and biological contexts. Therefore, an integrated analysis of PCD subtypes and their interplay within the atrial myocardium is critical for identifying novel molecular biomarkers and therapeutic targets.

In this study, we applied an integrative bioinformatics and machine-learning framework—encompassing 66 model combinations from 12 algorithms—to systematically identify key PCD-related genes in AF. Four hub genes (SGPL1, NPC2, PTGDS, and RCAN1) were used to construct a diagnostic model and a PCD-based risk score (PCDscore). Their expression patterns were validated in both AF cell models and peripheral blood mononuclear cells (PBMCs) from patients, confirming their clinical relevance. In addition, potential therapeutic candidates were explored, among which todralazine was identified as a potential therapeutic compound targeting these hub genes. This combined computational and experimental approach provides novel insights into the role of PCD in AF pathogenesis and offers promising biomarkers for precision diagnostics and targeted intervention.

Material and Methods

Dataset Collection and Processing

Gene expression data from patients with atrial fibrillation (AF) were acquired from the Gene Expression Omnibus (GEO) database, including GSE41177 (n = 38), GSE115574 (n = 59), GSE79768 (n = 26), and GSE282504 (n = 30). R version 4.3.1 was used for all data processing. The R package “GEOquery (version 2.70)” was used to retrieve the data. GSE41177 and GSE115574 were merged as the training set and processed to eliminate batch effects using the R package “sva (version 3.50).” Principal component analysis (PCA) was conducted to assess potential batch effects across datasets. Fourteen types of programmed cell death (PCD)-related genes were extracted from previous literature,¹⁷ and Genecards (<https://www.genecards.org/>) (Supplementary Table 1). Differentially expressed genes (DEGs) between AF and sinus rhythm (SR) groups were identified using the R package “limma (version 3.58),” with selection criteria of $|\log_2FC| > 0.25$ and P -value < 0.05 .

Consensus Clustering Analysis

Unsupervised consensus clustering was performed using the “ConsensusClusterPlus” package (v1.66). Similarity between samples was assessed using K-means clustering with Spearman distance. The optimal number of clusters (k) was determined by inspecting the cumulative distribution function (CDF) curves and delta area plots. Classification stability was further assessed using PCA.

Functional Enrichment Analysis

Gene Ontology (GO) and Kyoto Encyclopedia of Genes and Genomes (KEGG) enrichment analyses were conducted using the “clusterProfiler” package (v4.10). Gene Set Enrichment Analysis (GSEA) was performed with the “h.all.v2023.2.Hs.symbols” gene set from the Molecular Signatures Database (MSigDB). Normalized enrichment scores (NES) were calculated, and P-values were adjusted using the false discovery rate (FDR). Single-sample GSEA (ssGSEA) was implemented via the “Gene Set Variation Analysis (GSVA)” package (v1.50) to calculate GSVA scores for each sample.

Weighted Gene Co-Expression Network Analysis

Weighted Gene Co-expression Network Analysis (WGCNA) was conducted to identify gene modules associated with programmed cell death (PCD). Outlier samples were first removed through hierarchical clustering. A soft-thresholding power (β) was selected to meet the scale-free topology criterion ($R^2 > 0.8$). The resulting adjacency matrix was transformed into a topological overlap matrix (TOM). Co-expression modules containing a minimum of 50 genes were identified using dynamic tree cutting. Module–trait relationships were evaluated by calculating Pearson correlations between module eigengenes and sample traits. Genes from the module showing the strongest correlation with PCD were selected for subsequent analysis.

Machine Learning and Construction of Diagnostic Model

Twelve machine-learning algorithms—Elastic Net (Enet), Lasso, Ridge, Stepwise Generalized Linear Model (StepGLM), Support Vector Machine (SVM), Linear Discriminant Analysis (LDA), Generalized Linear Model Boosting (glmBoost), Partial Least Squares Regression for GLMs (plsRglm), Random Forest (RF), Generalized Boosted Regression Modeling (GBM), XGBoost, and Naive Bayes—were used in 66 model combinations to identify optimal diagnostic markers. Model performance was evaluated by the area under the receiver operating characteristic (ROC) curve (AUC) in the training set and two independent validation datasets (GSE79768, GSE282504). A diagnostic nomogram incorporating the four hub genes was developed using the “rms” package, with calibration curves and decision curve analysis (DCA) to assess accuracy and clinical benefit.

PCDscore Construction

Based on the expression of four hub genes, we established a PCDscore via PCA analysis:

$$\text{PCDscore} = \sum(PC1i + PC2i)$$

Where i is the expression of four key genes.

Immune Infiltration Analysis

Immune cell infiltration was estimated using CIBERSORT, xCell, and ssGSEA algorithms. Immune modulators from published datasets were compared between AF subtypes and visualized accordingly.

Prediction of Transcription Factors and microRNAs (miRNAs)

Transcription factors (TFs) and miRNAs associated with the 4 key genes were predicted by using databases of ChIPBase and ENCORI. The network diagrams were visualized by Cytoscape software (version 3.10.0).

Molecular Docking Simulation

Potential therapeutic compounds targeting the hub genes were identified using the Connectivity Map (CMap) database via Enrichr. The 2D structure of todralazine (CID:5501) was obtained from PubChem. Protein structures (NPC2: 5KWY; PTGDS: 3O22; RCAN1: 6UUQ; SGPL1: 8AYF) were retrieved from PDB database. The CB-Dock2 online tool¹⁸ was used to perform docking and visualization.

Cell Culture and AF Cell Model

The HL-1 rapid-pacing model provides a cardiomyocyte-intrinsic stressor mimicking pro-arrhythmic remodeling. Sham-paced wells served as negative controls. HL-1 atrial cardiomyocytes (Shanghai Institute of Biochemistry and Cell Biology) were cultured in DMEM/F12 with 10% FBS at 37 °C, 5% CO₂. Cells at passages (3–8) were used. For pacing, cells were seeded at $[0.8–1.2] \times 10^5$ cells·cm⁻² and allowed to adhere 12 h to reach ~70–80% confluence. AF cell model was established via rapid electrical pacing. HL-1 cells were paced with 5 ms, 5 Hz square-wave pulses (5 V) for 24 h by

utilizing a C-Pace100™ culture pacer. Sham controls were handled identically without current. To minimize edge effects, wells with electrode misalignment, detachment, or contamination were excluded a priori.

Clinical Samples and PBMC Isolation

All individuals in our study were recruited from the Department of Cardiology, the Central Hospital of Dalian University of Technology, as a single institution from September 2024 to May 2025. This study was conducted in accordance with the Declaration of Helsinki. The protocol was reviewed and approved by the Ethics Committee of the Central Hospital of Dalian University of Technology (Approval No: YN2024-134-26), and all participants provided written informed consent. Patients with persistent AF (episodes lasting >7 days without spontaneous termination, $n = 54$) were recruited from Central Hospital of Dalian University of Technology as the experimental group. Age- and body mass index (BMI)-matched healthy volunteers with no history of AF served as controls ($n = 47$). Inclusion criteria: age ≥ 18 years; diagnosed with persistent AF confirmed by electrocardiogram or Holter monitoring; provided written informed consent. Exclusion criteria: valvular AF; history of malignancy; heart failure (NYHA class III–IV); chronic kidney disease requiring dialysis; severe infection or autoimmune disease. The clinical details were shown in [Supplementary Table 2](#). Peripheral blood samples (3 mL) were collected in EDTA tubes, and PBMCs were isolated using a commercial kit (Solarbio, Beijing, China) within 2 h of collection, counted, and aliquots were stored at -80°C (RNA) or processed immediately for RNA extraction. Given the multi-tissue nature of AF and the PCD, we implemented a two-level validation strategy: (i) a cardiomyocyte-intrinsic readout using paced HL-1 atrial cells to test whether hub genes respond to pro-arrhythmic electrical stress and (ii) a circulating immune context readout using PBMCs from AF patients, considering the strong immune infiltration signal observed across CIBERSORT, xCell, and ssGSEA analyses and the macrophage enrichment in high-PCD score patients. This design allows us to probe both myocyte-centric and immune-inflammatory axes that jointly shape AF remodeling, while acknowledging that no single model fully captures the disease complexity.

RNA Extraction and Quantitative Real-Time PCR (qRT-PCR)

Total RNA was extracted from HL-1 cells or macrophages using an RNA isolation kit (Axygen, New York, USA). cDNA was synthesized from total RNA using a reverse transcription kit with genomic DNA removal capability (TOYOBO, Tokyo, Japan). qRT-PCR was performed using SYBR Green-based master mix (TOYOBO, Tokyo, Japan) under standard cycling conditions. β -actin was used as the internal reference gene. Relative gene expression levels were calculated using the $2^{-\Delta\Delta\text{Ct}}$ method. Primer sequences used in the analysis were provided in [Supplementary Table 3](#).

Western Blotting

HL-1 cells were lysed in RIPA buffer with protease/phosphatase inhibitors on ice. Lysates were clarified ($12,000\times\text{g}$, 10 min, 4°C), quantified by BCA, separated by SDS-PAGE, and transferred to PVDF. Membranes were blocked with 5% non-fat milk (TBST, 1 h, $20\text{--}25^{\circ}\text{C}$), incubated with primary antibodies against NPC2 and PTGDS (Proteintech, Wuhan, China) and against RCAN1 and SGLP1 (Cell Signaling Technology, MA, USA) overnight (4°C), washed, and probed with HRP-conjugated secondaries (1 h, $20\text{--}25^{\circ}\text{C}$). Signals were visualized by ECL.

ELISA

Conditioned media were collected and assayed using commercial ELISA kits following the manufacturer's instructions (Elabscience Biotechnology, Wuhan, Hubei, China).

Statistical Analysis

Statistical analyses were performed using R software (version 4.3.1). Methods for transcriptomic data processing are described in the corresponding section. Continuous variables are presented as mean \pm SD. Two-group comparisons used unpaired t-tests or Mann–Whitney U -tests as appropriate. Multiple-group comparisons used one-way ANOVA with Tukey post hoc or Kruskal–Wallis with Dunn post hoc. A P -value < 0.05 was considered statistically significant.

Results

Identification of Key PCD Types and Genes in AF

The flow chart of this study is shown in Figure 1. GSE41177 and GSE115574 datasets (37 SR and 60 AF samples) were merged after batch-effect removal, as validated by PCA (Supplementary Figure S1). Figure 2A illustrates that nine types of cell death showed significant differences between the SR group and AF group. Apoptosis, ferroptosis, autophagy and lysosome-dependent cell death were selected as key PCD types in AF using LASSO machine learning algorithm. (Figure 2B). Multivariate logistic regression identified 81 genes (Figure 2C) with diagnostic significance ($P < 0.05$), and intersection with the four key PCD types yielded 53 genes (Figure 2D), which were applied to construct the network (Figure 2E).

PCD-Related Subtypes in AF

Applying 53 diagnostic PCD genes, a consensus cluster analysis was conducted to classify AF patients into two AF subtypes. Optimal cluster stability (k) was determined via cumulative distribution function (CDF) analysis (Figure 3A). Delta area plots revealed a sharp decline in curve area beyond $k=2$ (Figure 3B). Differential expression genes (DEG) between two clusters were identified (Figure 3C). GO and KEGG analyses revealed that these DEGs were enriched in the regulation of cell-cell adhesion, activation of immune response, DNA-binding transcription factor binding, and in

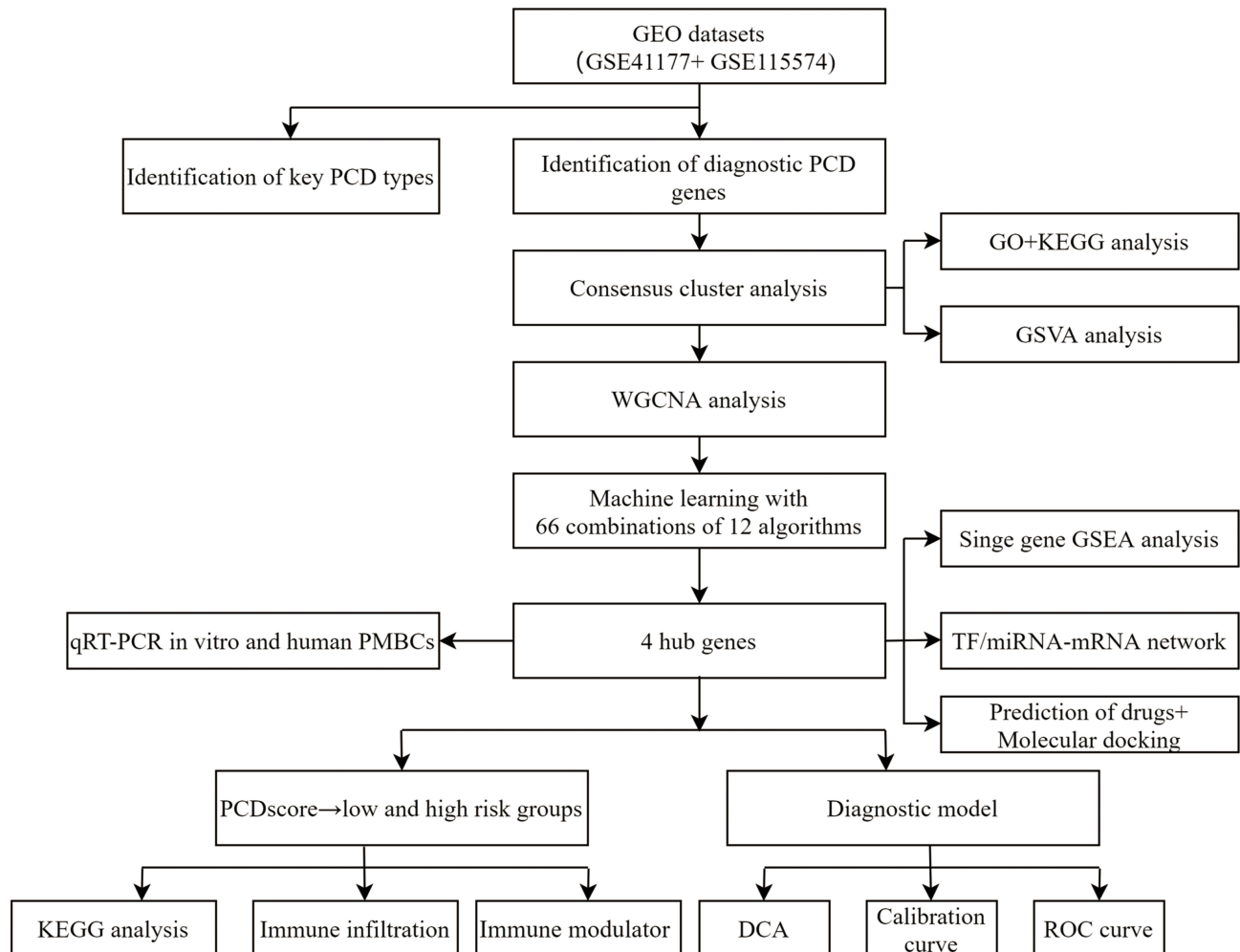


Figure 1 The flow chart of this study. Overview of data integration (GEO datasets GSE41177, GSE115574, GSE79768, GSE282504), machine-learning pipeline (12 algorithms; 66 combinations), hub-gene nomination, model building (nomogram, PCDscore), and experimental validation in HL-I cells and PBMCs.

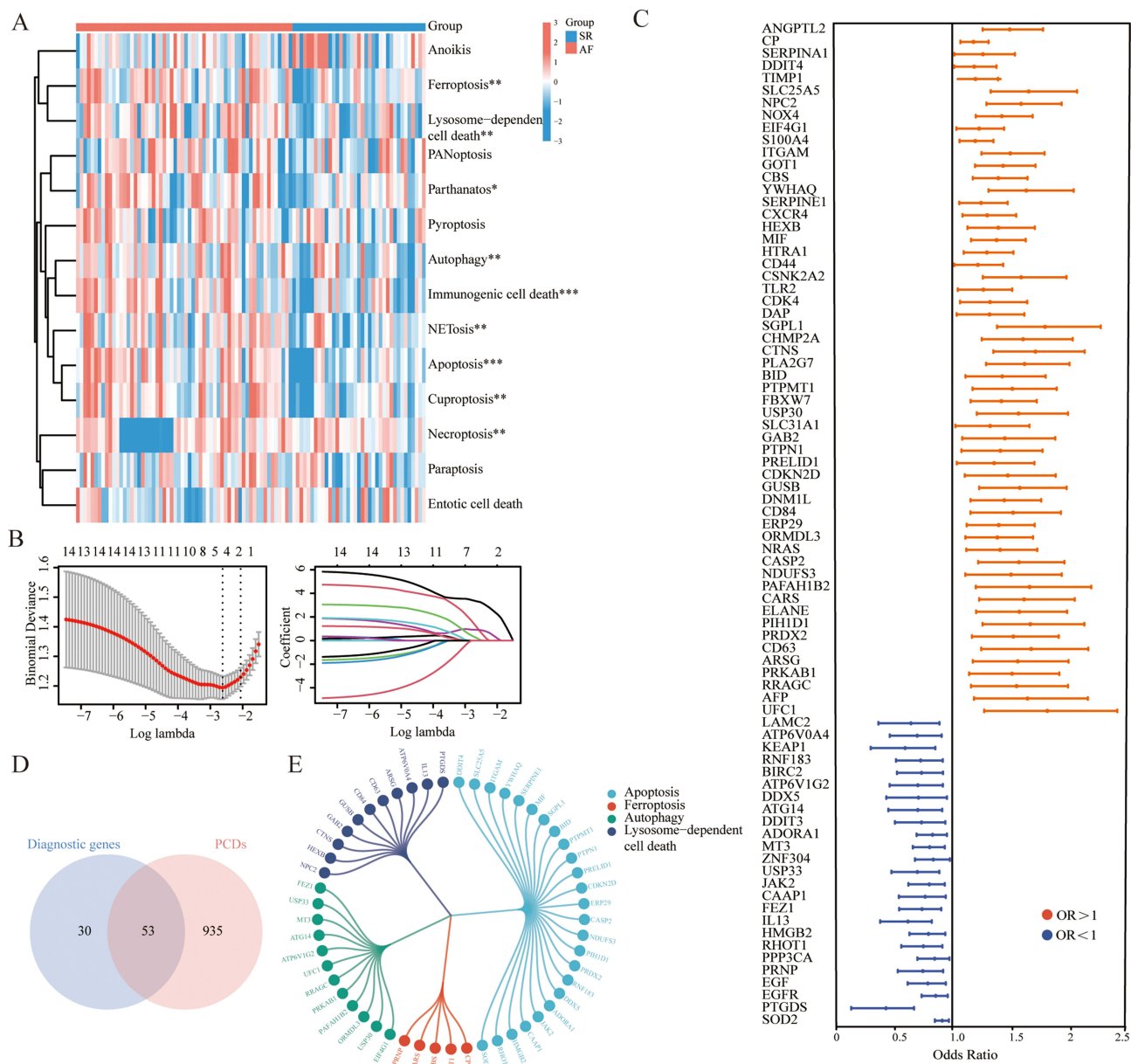


Figure 2 Identification of key PCD types and genes in AF. **(A)** Heatmap illustrating the GSVA scores for each type of PCD in SR and AF groups; **(B)** LASSO selection of PCD types associated with AF; **(C)** Multivariable logistic regression identifying diagnostic genes ($P < 0.05$); **(D)** Intersection of diagnostic genes with selected PCD types; **(E)** Network of 53 intersecting genes.

pathways of chemokine signaling, NOD-like receptor signaling and Hippo signaling (Figure 3D). GSVA analysis showed that the genes were enriched in pathways of JAK STAT3 signaling, apoptosis and PI3K AKT MTOR signaling, suggested these pathways may play key roles in AF development. (Figure 3E).

Weighted Gene Co-Expression Network Analysis and Identification of Key Modules Genes Associated with AF Progression

We used the WGCNA method to identify key module genes associated with AF progression. The level of R2 was set to 0.9 and soft threshold power was 7. (Figure 4A). Hierarchical clustering of module dissimilarity generated a dendrogram, identifying 14 distinct co-expression modules. (Figure 4B and C). The pink module showed the strongest negative correlation with cluster1 group ($r = -0.82, P < 0.001$). (Figure 4D). Figure 4E shows the intersection of the pink module and DEGs, resulting in a total of 16 genes, which were applied for subsequent machine learning.

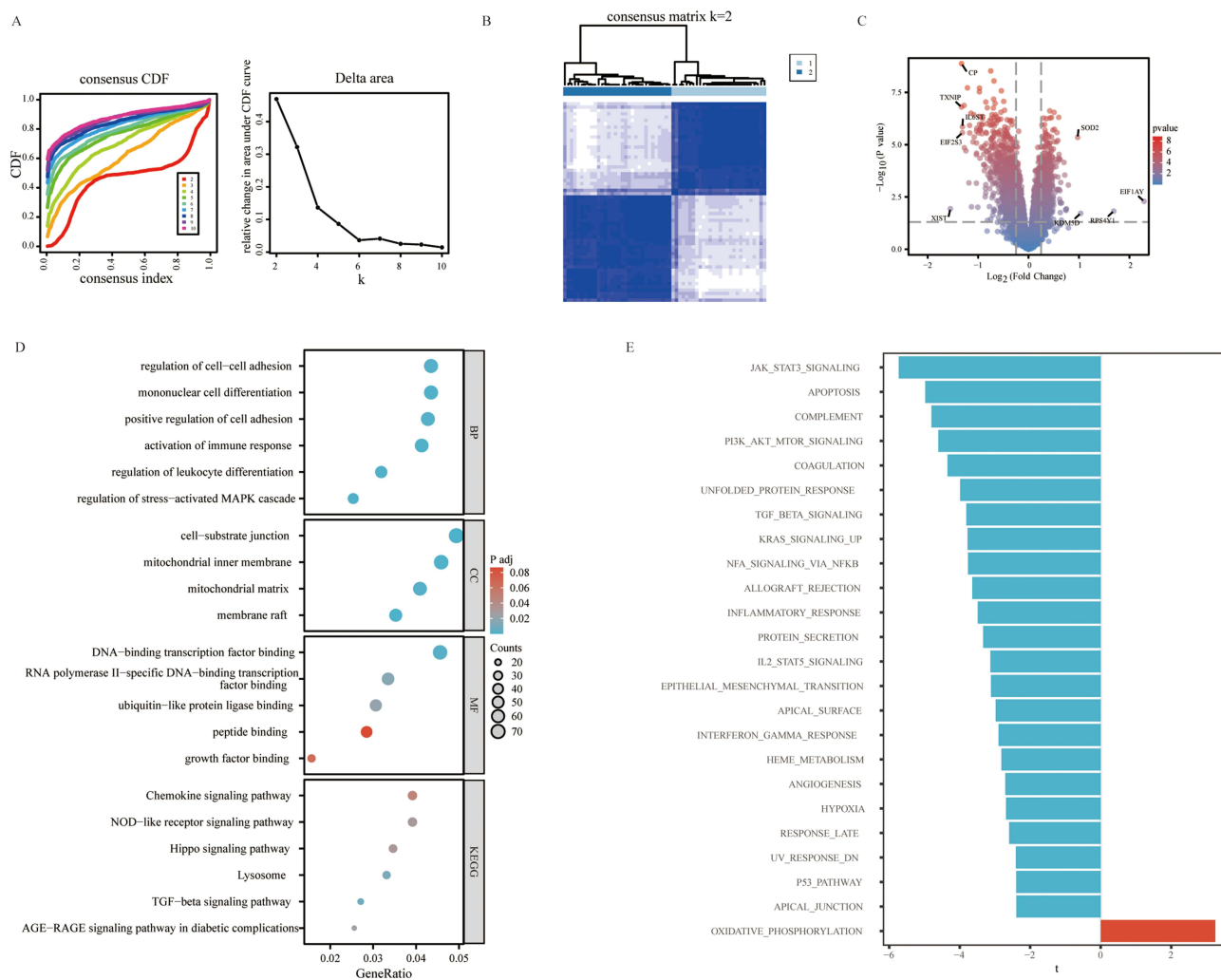


Figure 3 PCD-related subtypes in AF. **(A)** CDF curve for $k=2$; **(B)** The consensus score matrix of all samples when $k=2$; **(C)** Volcano plot showing DEGs between cluster 1 and cluster 2; **(D)** GO and KEGG enrichment analysis on the DEGs between cluster 1 and cluster 2; **(E)** GSEA analysis on the DEGs between the 2 clusters (Hallmark v2023.2).

Identification of Hub Genes Related to PCD with Diagnostic Value in AF Based on Integrative Machine Learning

To further explore the 16 gene features, we employed 66 combinations of 12 machine learning algorithms for variable selection and model development. Figure 5A showed the ranking of AUC values for all models. XGBoost, exhibiting the best performance, achieved an AUC of 0.983 in the training dataset, and AUCs of 0.688 (GSE79768), and 0.735 (GSE282504) in external validation datasets. Ultimately, our model selected four hub genes: SGPL1 (Sphingosine-1-Phosphate Lyase 1), NPC2 (NPC Intracellular Cholesterol Transporter 2), PTGDS (Prostaglandin D2 Synthase) and RCAN1 (Regulator of Calcineurin 1). Next, we calculated AUC values for each hub genes in the training dataset (Figure 5B) and validation datasets (Figure 5C and D), suggesting good diagnostic value for four hub genes.

Developing a Diagnostic Model Based on Hub Genes

Based on the four hub genes, we developed a predictive nomogram for the occurrence of AF. In the nomogram, each diagnostic signature corresponds to a distinct point value on its axis. The total score predicts the risk of AF (Figure 6A). The calibration curves of the diagnostic model closely approximated the ideal diagonal line, demonstrating excellent agreement between predicted and observed outcomes. (Figure 6B). The DCA curves showed the accuracy of the diagnostic model, which may provide clinical benefits for patients with AF (Figure 6C). The diagnostic model

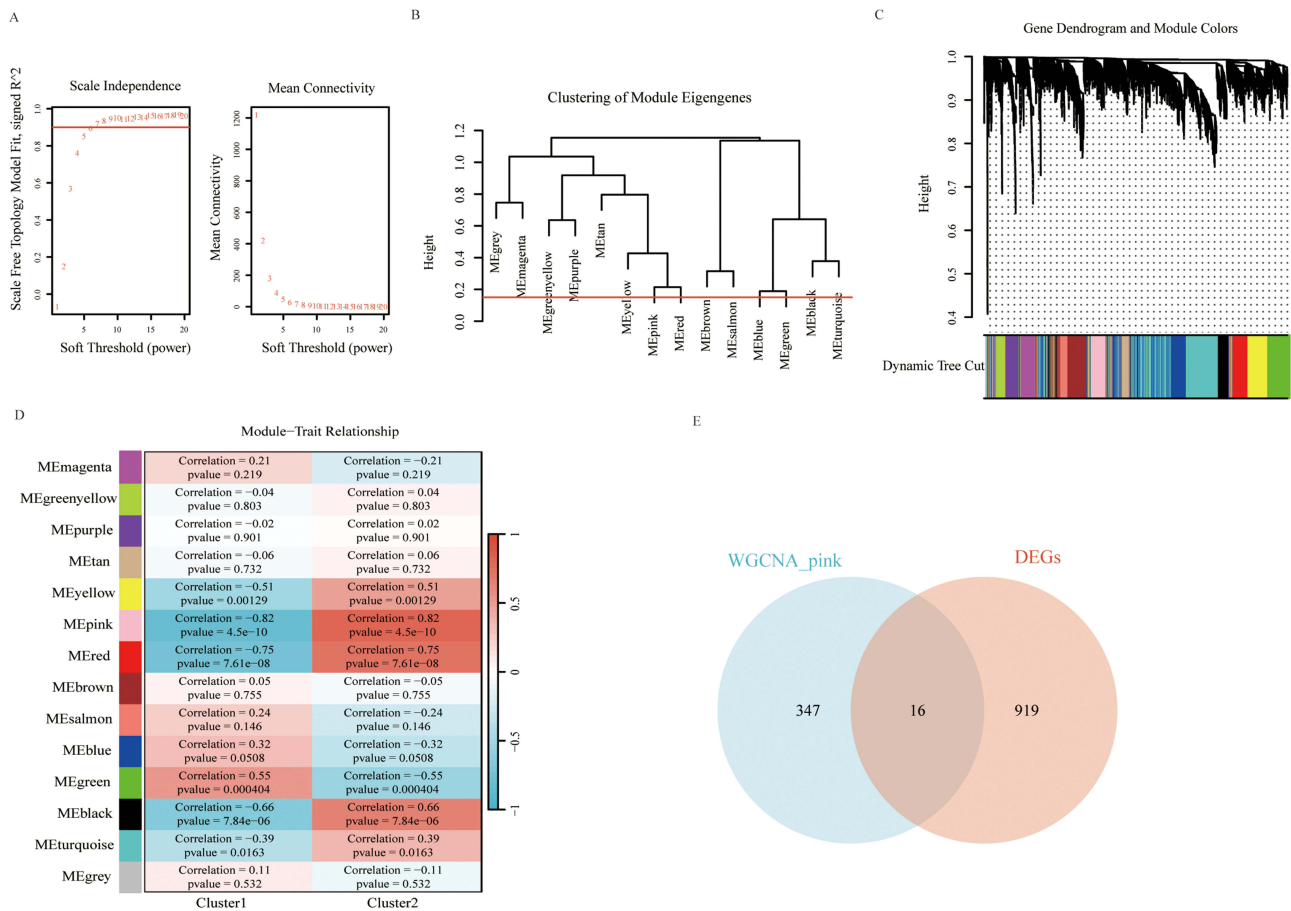


Figure 4 Identification of core genes in AF with WGCNA. **(A)** soft threshold power=7; **(B and C)** Module merging (cut height 0.15) and dendrogram; **(D)** Heatmap of correlation between key modules and AF clusters; **(E)** Overlap of pink-module genes with DEGs (n=16) forwarded to ML.

demonstrated excellent discriminative performance across both the training and validation cohorts, with an AUC of 0.933 in the training set, 0.982 (95% CI: 0.943–1.000) in the GSE79768 validation set, and 0.930 (95% CI: 0.841–1.000) in the GSE282504 validation set (Figure 6D–F). The nomogram model outperformed individual hub genes in ROC analysis, confirming its superior predictive utility for the occurrence of AF.

Functional Annotation and Immune Landscape of PCDscore

We established a scoring model, designated as the PCDscore, derived from the expression profiles of four hub genes. The detailed construction process is described in the methods section. Based on the median PCDscore, AF patients were classified into high-risk and low-risk groups (Figure 7A). We identified 908 DEGs among two groups, of which 574 were upregulated and 334 were downregulated. KEGG analysis revealed that the DEGs were primarily enriched in activation of immune response, ERK1 and ERK2 cascade, positive regulation of MAPK cascade, PI3K-Akt signaling pathway and MAPK signaling pathway (Figure 7B). Next, we use CIBERSORT, ssGSEA and xCell algorithms to analyze the immune landscape between two groups. We observed significantly distinct immune cell distribution between the two groups, with elevated infiltration levels in the high-risk group (Figure 7C). Notably, macrophage enrichment was significantly elevated across 3 algorithms. Furthermore, the immune modulators were higher in the high-risk group than in the low-risk group (Figure 7D). Correlation analysis demonstrated that the PCDscore, along with NPC2 and SGPL1, was significantly associated with numerous immune cell populations, prominently activated CD8⁺ T cells, Gamma delta T cells, macrophages, and myeloid-derived suppressor cells (MDSCs) (Figure 7E). In conclusion, high-risk group patients displayed elevated immune infiltration and immunoregulatory molecules, which may contribute to AF progression.

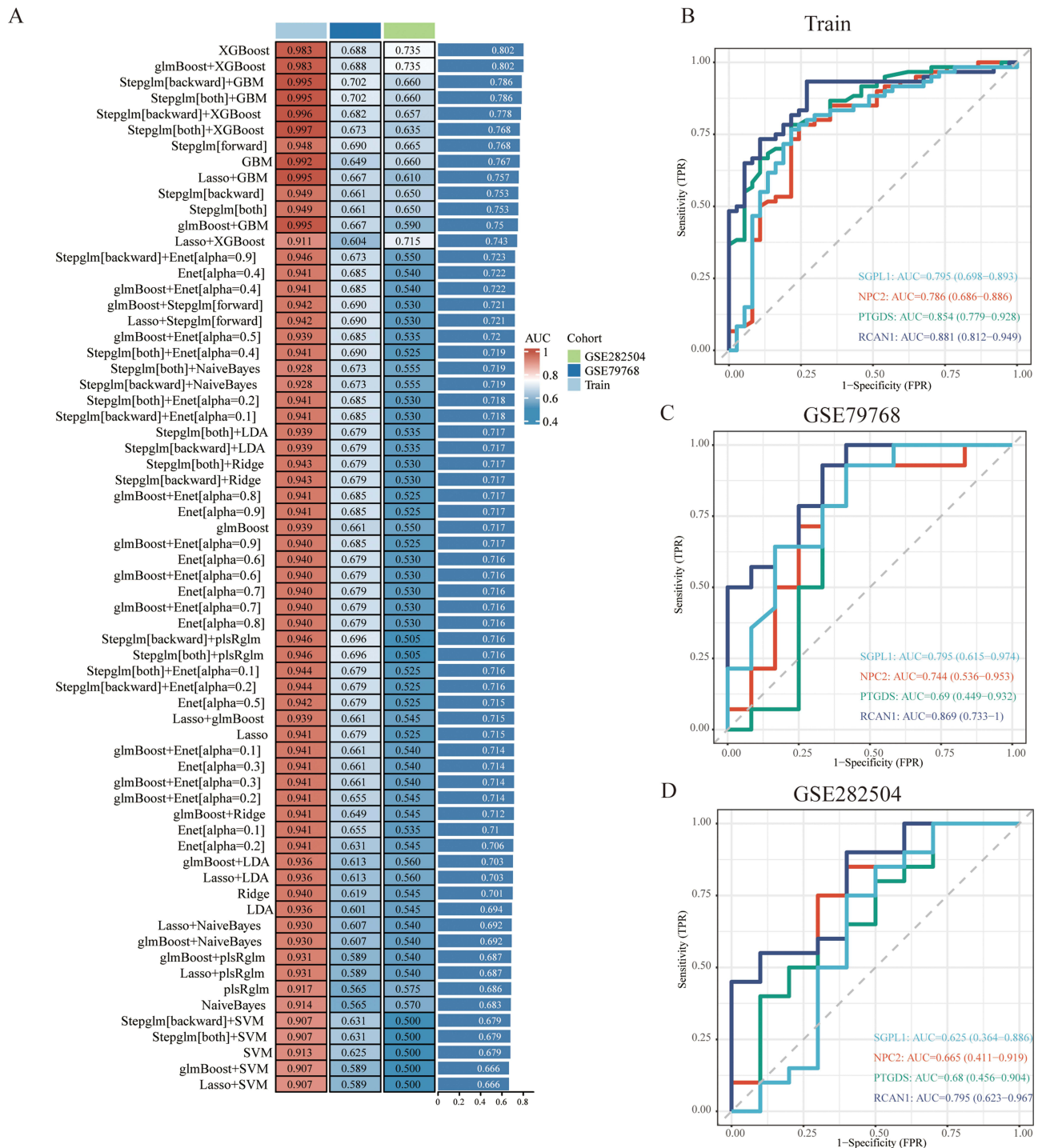


Figure 5 Identification of hub genes by machine learning. **(A)** A total of 66 combinations of 12 machine learning algorithms were constructed to identify hub genes; The area under the curve (AUC) for each model was evaluated across three independent datasets; **(B–D)** The AUC of four hub genes in training dataset and validation datasets.

Single-Gene GSEA of Hub Genes

We used a single-gene GSEA method to further explore the biological functions and pathways of hub genes. We found that the hub genes were associated with biological processes, such as chemokine signaling pathway, tricarboxylic acid (TCA) cycle, p53 signaling pathway, gluconeogenesis, mitochondrial translation and oxidative phosphorylation. These results indicated that the hub genes may serve key roles in the regulation of cell death and metabolism (Figure 8A–H).

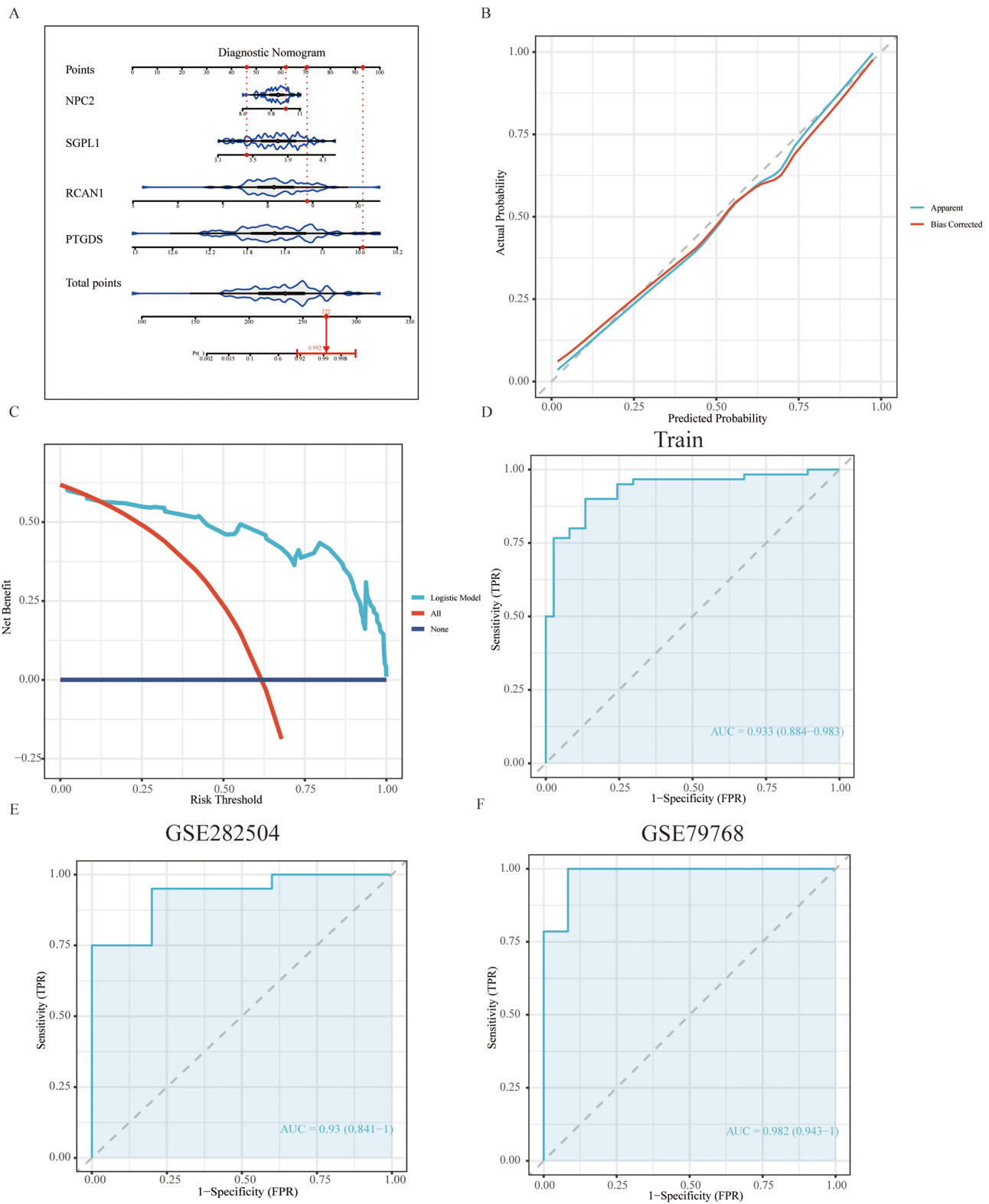


Figure 6 Developing a diagnostic model based on hub genes. **(A)** A diagnostic nomogram incorporating four hub genes was developed. Each gene was assigned a specific score, and the cumulative score derived from all four genes was used to estimate the risk of AF; **(B)** Calibration curve assessed predicted–observed concordance, validating the nomogram’s accuracy; **(C)** Decision curve analysis (DCA) quantified the nomogram’s clinical benefit for AF diagnosis; ROC curves illustrating the nomogram’s predictive accuracy for AF in the training set **(D)** and validation datasets **(E and F)**.

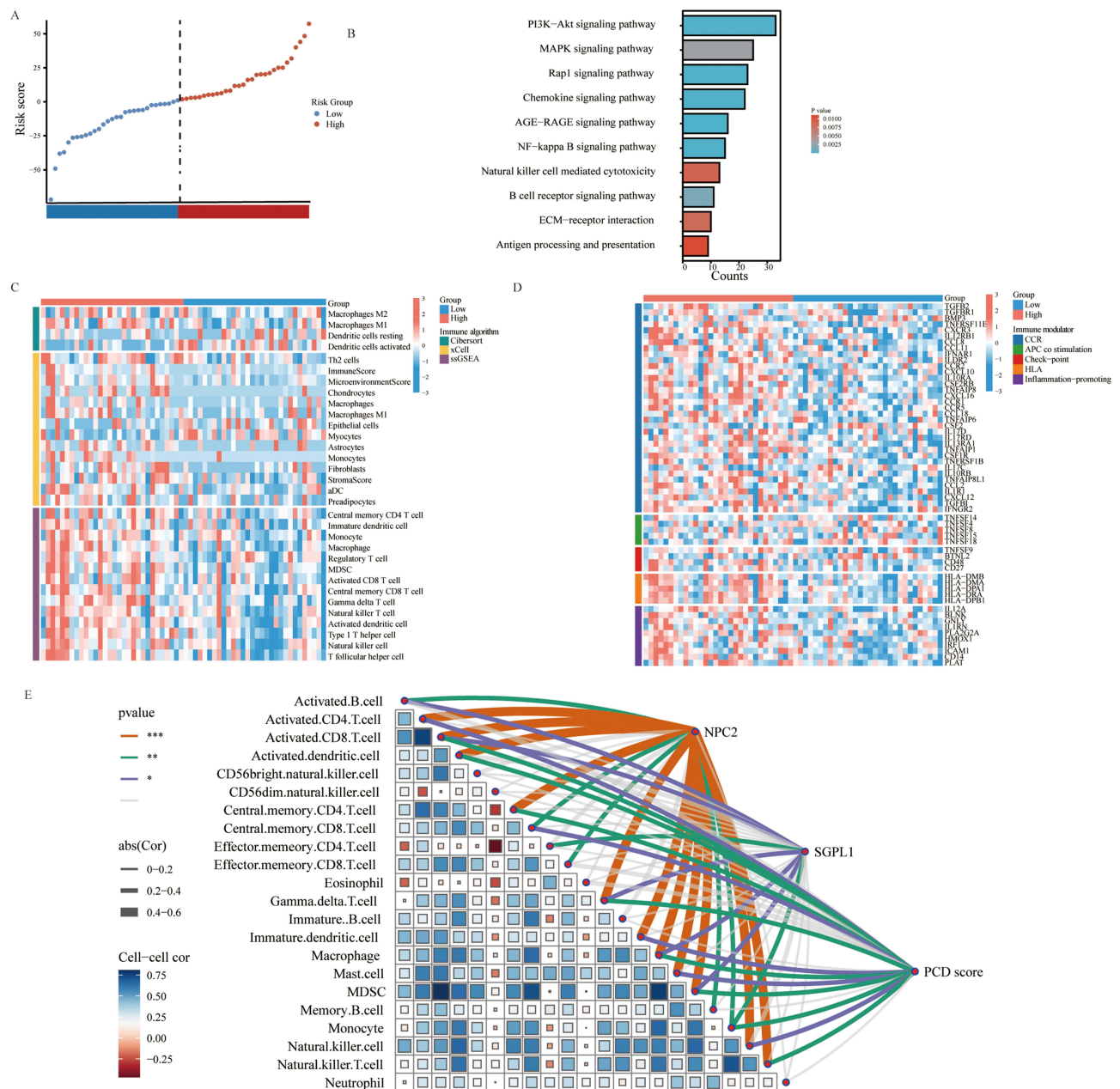


Figure 7 Functional annotation and immune landscape of PCDscore. **(A)** Distribution of PCDscores of AF patients; **(B)** The KEGG functional enrichment of differential genes between high and low risk groups; **(C)** Heatmap illustrating the immune landscape between the high and low risk groups; **(D)** Heatmap illustrating the immune modulators between the two high and low risk group; **(E)** Correlation matrix between PCDscore, NPC2, SGPL1 and various immune cell types.

Construction of Regulatory Network of Hub Genes

To explore upstream molecular regulators of hub genes, we performed a TF/miRNA-mRNA network analysis. Forty-two Potential miRNAs, with a degree of ≥ 2 , were identified through ENCORI database (Figure 9A). miR-7-5p was a common miRNA for NPC2, RCAN1 and PTGDS. Through the ChIPBase database, we identified 26 TFs with a degree ≥ 2 (Figure 9B). YY1 was a common TF for NPC2, RCAN1 and SGPL1.

Prediction of Drugs and Molecular Docking for Hub Genes

Potential therapeutic drugs targeting hub genes were identified via the CMAP database. Figure 10A displays the top 10 candidates by combined score, with todralazine emerging as the top-scoring repurposing candidate for further evaluation.

Accordingly, we performed docking against the four hub proteins (Figure 10B–E). The Vina scores of todralazine with the four hub genes were less than -5 (Table 1), indicating robust binding affinities.

Experimental Validation of Hub Genes in vitro and Human Sample

Tachypacing of HL-1 cardiomyocytes is a widely used, canonical in vitro AF model. Prior work showed time-dependent up-regulation of Hspa1a (HSP70), Nppa, and Nppb in paced HL-1 cells.^{19,20}

Consistent with this paradigm, we verified increased HSPA1A/NPPA/NPPB by qPCR and elevated ANP/BNP in supernatants by ELISA (Supplementary Figure S2). We then quantified the four hub genes in paced HL-1 cells by qRT-PCR and Western blot: SGPL1, NPC2, and RCAN1 were significantly up-regulated, whereas PTGDS was down-regulated (Figure 11A–D and G). In PBMCs, NPC2 and SGPL1 were higher in AF patients than in controls (Figure 11E and F).

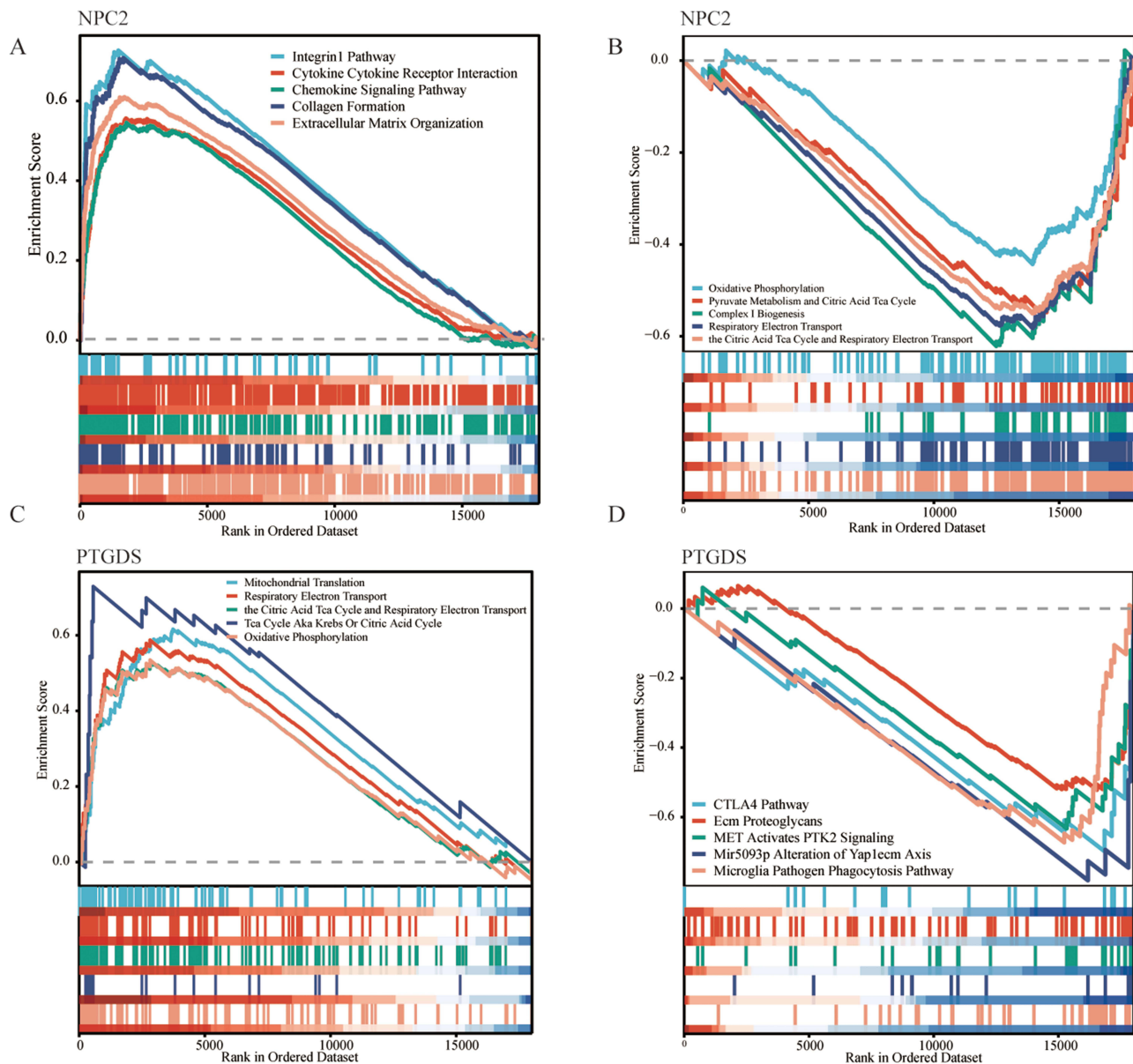


Figure 8 Continued.

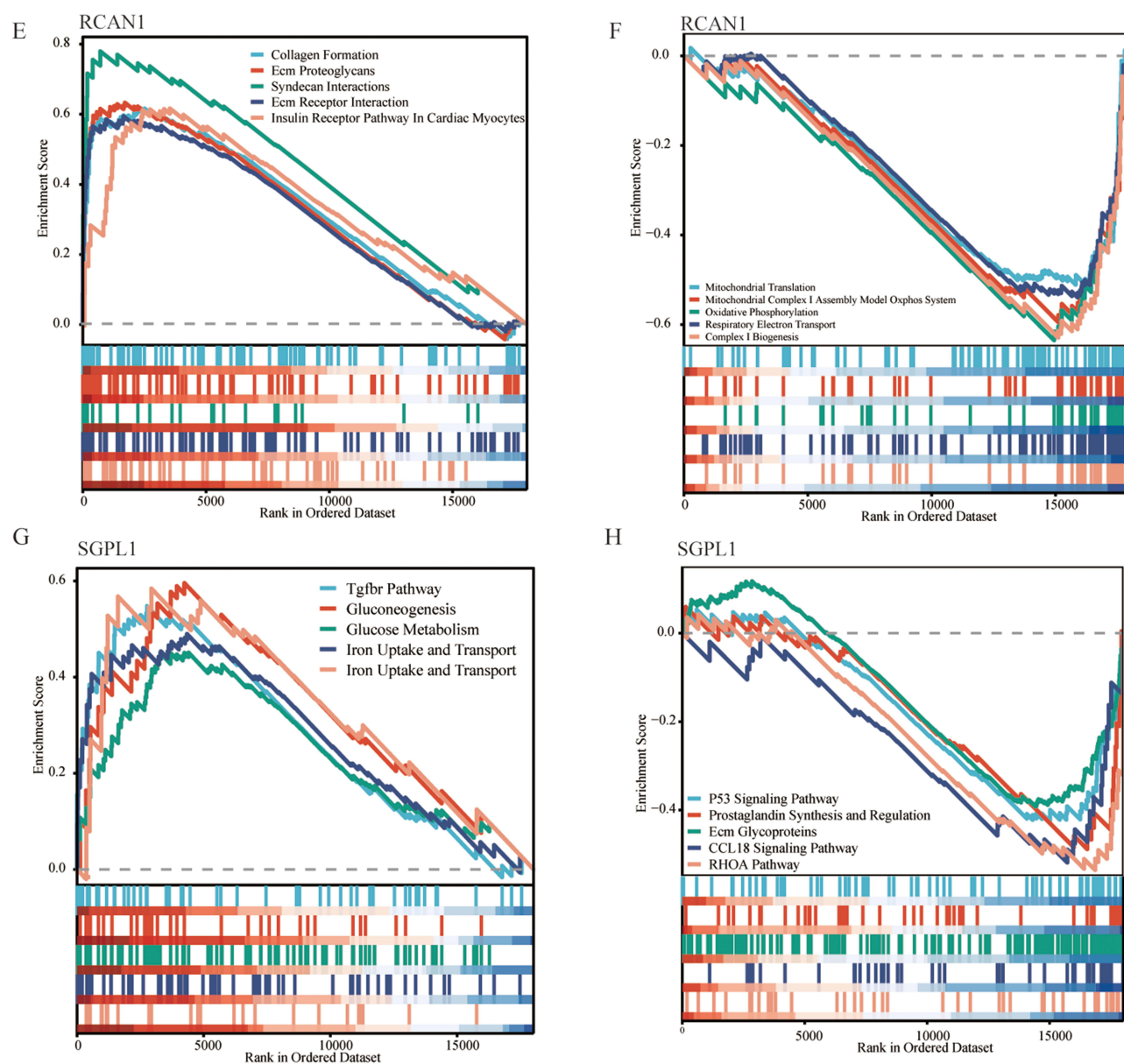


Figure 8 Single-gene GSEA of hub genes. (A–H) represents the signaling pathway associated with NPC2 (A and B), PTGDS (C and D), RCAN1 (E and F) and SGPL1 (G and H).

Discussion

Atrial fibrillation (AF) remains a major contributor to stroke, heart failure, and all-cause mortality.¹ Despite significant advancements in pharmacological therapy and catheter ablation techniques, clinical efficacy remains suboptimal and personalization is lacking.⁵ These limitations underscore the urgent need to elucidate the underlying molecular mechanisms of AF—particularly those involving programmed cell death (PCD) pathways. A deeper understanding of these mechanisms is essential for early detection, refined risk stratification, and the development of personalized therapeutic strategies to mitigate disease progression and improve clinical outcomes.

In this study, we systematically identified four PCD-related hub genes—SGPL1, NPC2, PTGDS, and RCAN1—associated with atrial fibrillation (AF) through integrative bioinformatics and machine-learning approaches. Based on these hub genes, we constructed a diagnostic nomogram with robust predictive performance. Furthermore, we developed a PCDscore that effectively stratified patients into high- and low-risk subgroups. Notably, the high-risk group exhibited

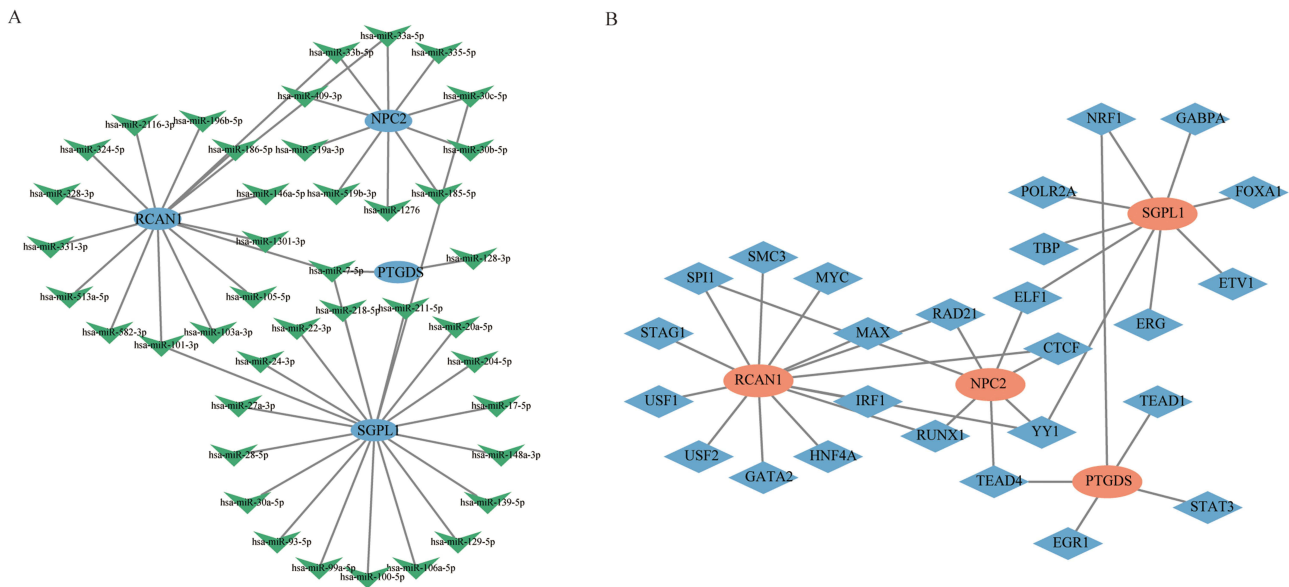


Figure 9 Construction of regulatory network of hub genes. **(A)** Interaction network of miRNAs and hub genes; **(B)** Interaction network of TFs and hub genes.

significantly elevated immune cell infiltration and immune-modulator dysregulation, features associated with more severe disease progression. Experimental verification in AF cell models and PBMCs from AF patients confirmed the bioinformatics findings, thereby reinforcing their clinical relevance.

Our study highlights four key PCD mechanisms—apoptosis, autophagy, ferroptosis, and lysosome-dependent cell death—as critical contributors to AF pathogenesis. Apoptosis is a caspase-dependent process leading to controlled cellular dismantling; in AF, it is promoted by epicardial fat-derived extracellular vesicles carrying pro-inflammatory and profibrotic mediators such as cytokines and miR-146b,²¹ and by β -hydroxybutyrate-induced mitochondrial dysfunction,²² thereby contributing to fibrosis and arrhythmogenesis. Autophagy plays a dual role in AF. Basal autophagy acts as a cardioprotective mechanism by removing damaged mitochondria via mitophagy and maintaining protein homeostasis, potentially preventing AF onset. However, excessive or dysregulated autophagy—induced by rapid electrical pacing, inflammation, neutrophil extracellular traps (NETs), or N-palmitoyl glycine—may accelerate AF progression.¹⁶ This occurs through degradation of essential cardiac proteins such as Cx43, L-type calcium channels, and NRAP, contributing to both electrical and structural remodeling. Ferroptosis, a form of iron-dependent cell death characterized by lipid peroxidation and GPX4 suppression, has also been implicated in atrial remodeling. Pharmacological inhibition of ferroptosis by agents such as icariin and ferrostatin-1 has been shown to attenuate ethanol-induced AF via the SIRT1–Nrf2–HO-1 signaling pathway, highlighting ferroptosis as a promising therapeutic target.¹⁴ Lysosome-dependent cell death, initiated by lysosomal membrane permeabilization and characterized by cytosolic release of cathepsins and redox-active iron,^{23,24} may represent an underexplored mechanism in AF. This process can lead to proteolytic degradation and cell death, suggesting a possible role in atrial tissue injury and electrical instability. Further investigation into this pathway may uncover novel therapeutic strategies.

Among these hub genes, SGPL1 and NPC2 have not, to our knowledge, been reported or systematically examined in the context of AF, highlighting a novel mechanistic link between PCD and AF revealed by this study. SGPL1 encodes sphingosine-1-phosphate lyase, which irreversibly degrades S1P, a lipid signaling molecule involved in immune

Table I Vina Score of Todalazine to Four Hub Genes

Gene	PTGDS	NPC2	SGPL1	RCAN1
Vina Score	-6.4	-8	-7.1	-6.6

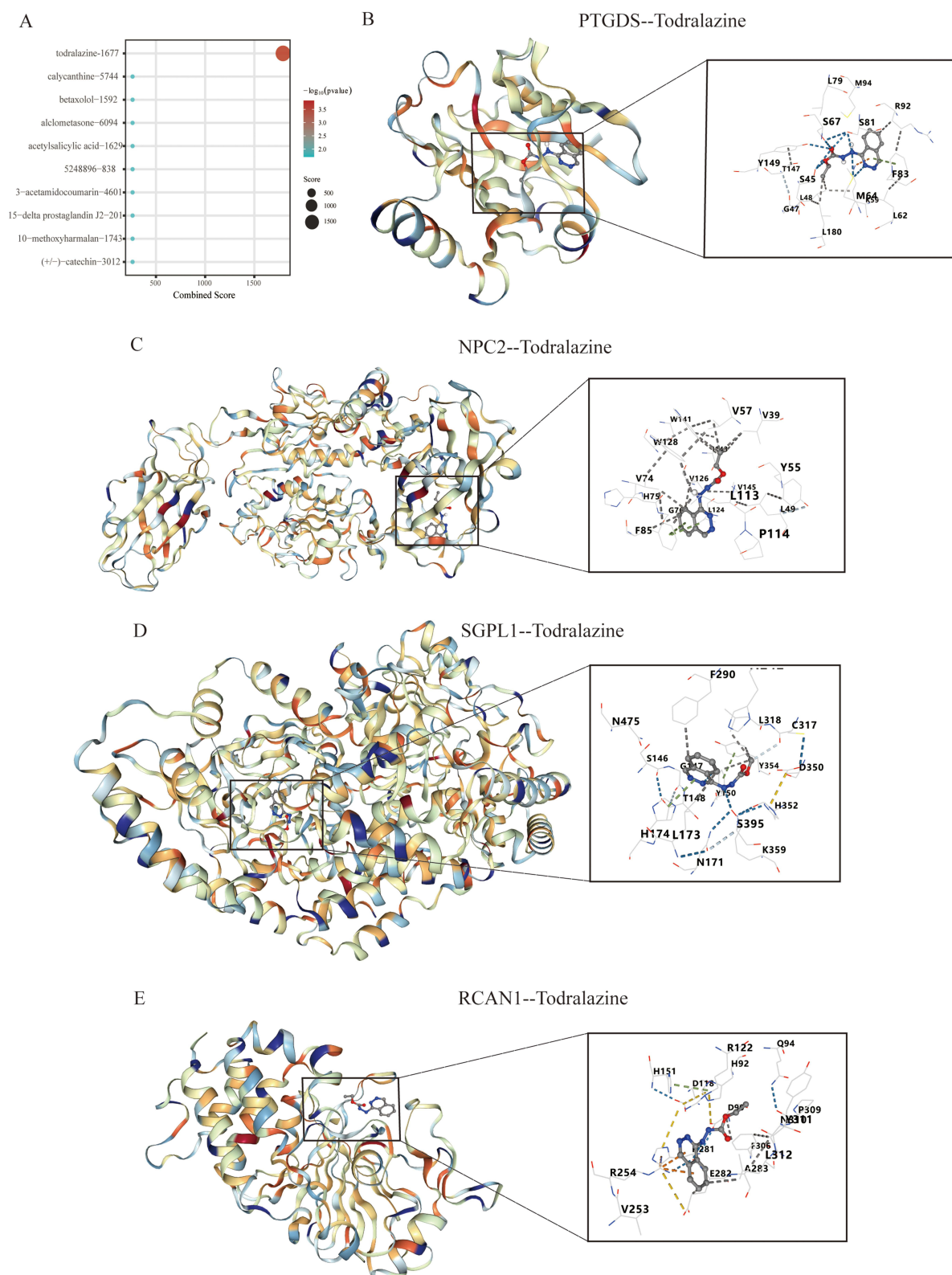


Figure 10 Prediction of drugs and molecular docking. **(A)** The top 10 candidate drugs were predicted for hub genes using CMAP database. **(B–E)** Todralazine docking to NPC2 (PDB 5KWY), PTGDS (3O22), RCAN1 (6UUQ), and SGPL1 (8AYF) using CB-Dock2. Reported Vina scores (Table 1) indicate favorable binding (<-5).

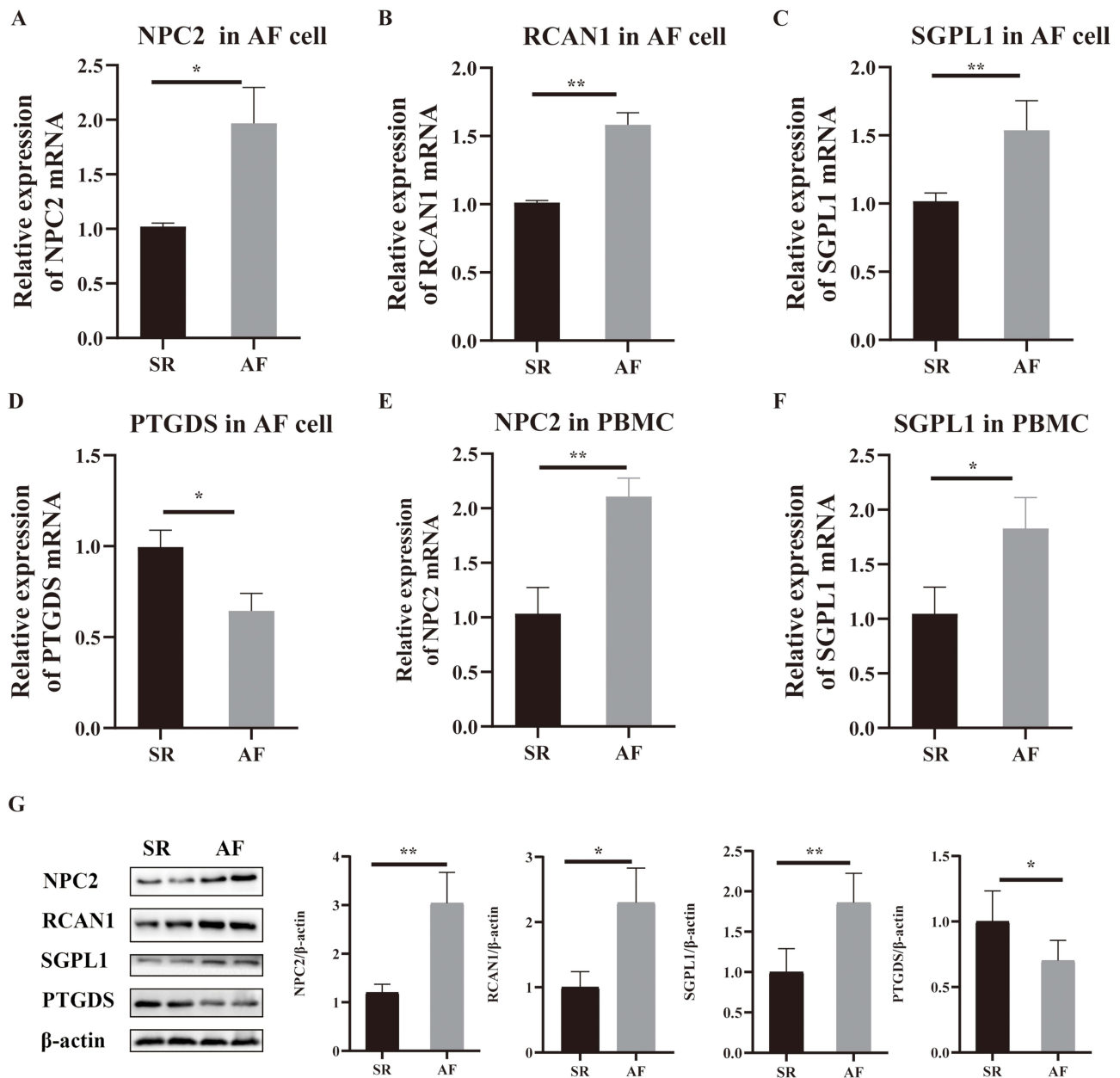


Figure 11 Experimental validation in HL-1 cells and human PBMCs. qRT-PCR analysis of NPC2 (A), RCAN1 (B), SGPL1 (C) and PTGDS (D) expression in AF cell models; qRT-PCR analysis of NPC2 (E) and SGPL1 (F) in PBMCs from AF patients and healthy controls. (G) Western blot analysis of NPC2, RCAN1, SGPL1 and PTGDS expression in AF cell models. * $P < 0.05$; ** $P < 0.01$.

regulation, mitochondrial function, and cell survival.²⁵ SGPL1 deficiency results in S1P accumulation, impairing autophagy, disrupting germ cell development via NPR2/p21 pathways, and contributing to neuroinflammation and immune cell activation.²⁶ SGPL1 mutations are associated with sphingosine phosphate lyase insufficiency syndrome, a systemic disorder featuring neurological deficits and immune dysfunction.²⁷ SGPL1 deficiency leads to S1P accumulation, impairing autophagic flux and promoting inflammatory cell infiltration, processes that may exacerbate atrial fibrosis and electrical instability. Our finding that SGPL1 is significantly upregulated in AF suggests that altered S1P metabolism may be a driver of PCD-related remodeling in atrial tissue.

NPC2 encodes a lysosomal cholesterol-binding protein that cooperates with NPC1 to mediate intracellular cholesterol transport.²⁸ Beyond its role in lipid homeostasis, NPC2 dysregulation can trigger lysosomal membrane permeabilization, releasing proteases such as cathepsins that initiate lysosome-dependent cell death. In immune contexts, NPC2 modulation

affects antigen presentation and inflammatory signaling, both of which may influence the pro-inflammatory microenvironment in AF.^{29–32} The upregulation of NPC2 observed in both AF cell models and patient PBMCs supports its potential role in coupling lipid metabolism, immune activation, and PCD in AF pathogenesis.

AF is characterized by considerable clinical and molecular heterogeneity, which contributes to highly variable responses to standard therapies.^{33,34} Recent research has highlighted the role of immune remodeling—particularly macrophage-driven inflammation—in the maintenance and progression of AF.³⁵ Pro-inflammatory CCR2⁺ macrophages infiltrate atrial tissue and contribute to electrical and structural remodeling through secretion of cytokines such as IL-1 β , TNF- α , and TGF- β . These inflammatory mediators promote atrial fibrosis and arrhythmogenicity.³⁶ In our study, the immune landscape analysis revealed that high-risk group patients exhibited pronounced infiltration of macrophages, CD8⁺ T cells, and myeloid-derived suppressor cells (MDSCs), along with dysregulated immune modulators. These observations align with previous studies showing that immune remodeling, particularly macrophage-driven inflammation, contributes to atrial structural changes and arrhythmogenesis. This suggests that PCD-related molecular alterations may potentiate immune-mediated atrial remodeling, providing a mechanistic link between molecular death pathways and clinical AF phenotypes.

Atrial fibrillation (AF) emerges from coupled electrical and structural remodeling driven by metabolic, mitochondrial, and inflammatory stress.³⁷ Major programmed cell-death (PCD) subtypes provide convergent routes to these changes: apoptosis and necroptosis impair myocyte viability and tissue integrity,³⁸ pyroptosis releases IL-1 β /IL-18 and DAMPs that amplify myeloid recruitment and cytokine signaling,³⁹ ferroptosis reflects lipid-ROS stress that destabilizes membranes and conduction;¹⁵ autophagy-related death intersects with lysosomal flux and proteostasis.⁴⁰ Together, these pathways promote conduction heterogeneity, Ca²⁺ cycling abnormalities, and fibro-inflammatory remodeling, all permissive to AF maintenance. Our data fit this framework at two levels. First, HL-1 rapid pacing recapitulates a cardiomyocyte-intrinsic PCD/stress signature, with RCAN1 \uparrow (calcineurin–NFAT stress⁴¹), SGPL1 \uparrow (sphingolipid/S1P turnover⁴²), NPC2 \uparrow (lysosomal–cholesterol trafficking/stress⁴⁰), and PTGDS \downarrow (reduced PGD2 anti-inflammatory tone⁴³), consistent with PCD-linked metabolic/lysosomal stress. Second, PBMC findings and immune-deconvolution support myeloid enrichment, aligning with DAMP/cytokine-driven atrial–immune cross-talk.³⁶ Thus, while our study demonstrates association rather than causality, the gene-level signals align with a biologically coherent PCD \rightarrow inflammation/fibrosis \rightarrow AF axis. We therefore describe SGPL1, NPC2, RCAN1, PTGDS as candidate biomarkers anchored to this PCD framework, and we outline targeted *in vitro/in vivo* validation to test causality in future work.

From a translational perspective, our drug-repurposing analysis identified todralazine—an established antihypertensive agent—as a potential compound targeting all four hub proteins, with molecular docking indicating strong-binding affinities. Given its known safety profile, todralazine may represent a feasible candidate for modulating PCD-related pathways in AF. This finding is consistent with recent advances in drug repurposing for cardiovascular diseases.^{44,45} While the current evidence is limited to *in silico* docking, these results provide a rationale for targeted preclinical studies to evaluate whether todralazine can influence PCD-driven atrial remodeling. Such investigations could help determine its potential role as an adjunctive therapeutic option for AF patients, particularly those classified as high-risk by our PCDscore model.

Our multi-omics analyses and validations support a working model in which PCD-linked metabolic–lysosomal remodeling in atrial myocytes amplifies danger signaling (eg, altered sphingolipid/lysosomal flux, oxidative stress), which in turn promotes myeloid recruitment and activation in the atrial micro-environment. The high-PCDscore subgroup showed concordant macrophage enrichment and immune-modulator dysregulation across three deconvolution algorithms, suggesting that PCD-primed cardiomyocytes may shape an inflammatory feed-forward loop with atrial macrophages. In this framework, HL-1 pacing captures the cardiomyocyte-intrinsic arm (PCD/metabolic stress), whereas PBMC assays reflect the systemic immune axis that correlates with atrial inflammation. This dual-axis rationale justifies the feasibility of using a single cardiomyocyte model plus human PBMCs to orthogonally validate bioinformatic signals at this stage, while recognizing the need for *in vivo* confirmation.

Nevertheless, this study has several limitations. First, although HL-1 tachypacing and patient PBMCs provide orthogonal validation across myocyte-intrinsic and immune compartments, they do not establish causality for the four hub genes. We will address this with (i) rodent AF models testing whether modulation of SGPL1, NPC2, PTGDS, and

RCAN1 alters AF inducibility/duration, atrial fibrosis, and immune infiltration; (ii) myeloid–cardiomyocyte co-culture and conditioned-medium experiments to probe bidirectional signaling; and (iii) loss-/gain-of-function perturbations (siRNA/CRISPRa and pharmacologic tools targeting the S1P–SGPL1 and lysosomal–NPC2 axes) to dissect the PCD subtypes implicated here. Second, public datasets lacked harmonized clinical covariates (eg, AF subtype, comorbidities, medications), limiting risk adjustment and generalizability; to overcome this, we are assembling prospective, deeply phenotyped cohorts and conducting *in vivo* studies using atrial AAV perturbation. Third, this study is not a diagnostic trial. Demonstrating clinical utility will require a prospective, adjudicated cohort with pre-specified decision thresholds, independent verification against ECG/Holter-based diagnoses, calibration, and decision-curve analyses. Finally, the current PCDscore is biologically informative but omits clinical covariates because these variables were incomplete and non-harmonized across cohorts; future iterations will integrate age/sex and key physiological variables, undergo recalibration and external validation, and quantify net clinical benefit before any clinical deployment.

Conclusion

In conclusion, this study identified and validated four PCD-related hub genes—SGPL1, NPC2, PTGDS, and RCAN1—strongly associated with AF. Based on these genes, we established a high-performance diagnostic model and derived a PCDscore that robustly reflected immune and molecular heterogeneity; notably, high-risk patients displayed pronounced immune cell infiltration and marked dysregulation of immune modulators. Clinically, these findings provide a foundation for precision diagnostics and individualized risk assessment in AF, as well as a rationale for developing targeted interventions aimed at modulating PCD pathways.

Data Sharing Statement

All public transcriptomic datasets analyzed in this study are available from GEO under accessions GSE41177, GSE115574, GSE79768, and GSE282504. Additional data supporting the findings of this study are available from the corresponding author upon reasonable request.

Ethics Statement

Studies involving human data were reviewed and approved by the Ethics Committee of the Central Hospital of Dalian University of Technology (Approval No.: YN2024-134-26; approval date: 2024-10-21). All participants provided written informed consent prior to enrollment and sample collection. The research complied with the principles of the Declaration of Helsinki (2013). No identifiable personal data or images are included; consent for publication of de-identified data was obtained.

Author Contributions

Hongbo Peng: Conceptualization, Data curation, Formal analysis, Investigation, Methodology, Project administration, Software, Validation, Visualization, Writing – original draft. Writing – review & editing. Zhenwei Xia: Conceptualization, Data curation, Formal analysis, Investigation, Methodology, Project administration, Software, Validation, Visualization, Funding acquisition, Writing – original draft. Yangyang Zhao: Conceptualization, Investigation, Project administration, Methodology, Software, Writing – original draft. Di Xie: Conceptualization, Data curation, Formal analysis, Investigation, Methodology, Project administration, Software, Validation, Visualization, Supervision, Writing – review & editing. All authors gave final approval of the version to be published, agreed to submit this paper to the Journal of Inflammation Research, and agreed to be accountable to the contents of this paper.

Acknowledgments

The authors are grateful to all study participants for their involvement. We also acknowledge the Gene Expression Omnibus (GEO) database for granting access to the publicly available datasets that supported this work.

Funding

This study was supported by the Scientific Research Project of Dalian Medical Key Specialty “Climbing Peak Plan” (grant number 2024ZZ066).

Disclosure

The author(s) report no conflicts of interest in this work.

References

1. Brundel B, Ai X, Hills MT, Kuipers MF, Lip G, de Groot N. Atrial fibrillation. *Nat Rev Dis Primers*. 2022;8(1):21. doi:10.1038/s41572-022-00347-9
2. Al-Khatib SM. Atrial Fibrillation. *Ann Intern Med*. 2023;176(7):ITC97–ITC112. doi:10.7326/AITC202307180
3. Newman JD, O'Meara E, Böhm M, et al. Implications of Atrial Fibrillation for Guideline-Directed Therapy in Patients With Heart Failure: JACC State-of-the-Art Review. *J Am Coll Cardiol*. 2024;83(9):932–950. doi:10.1016/j.jacc.2023.12.033
4. Iwamiya S, Ihara K, Nitta G, Sasano T. Atrial Fibrillation and Underlying Structural and Electrophysiological Heterogeneity. *Int J Mol Sci*. 2024;25(18). doi:10.3390/ijms251810193
5. Al-Kaisey AM, Parameswaran R, Bryant C, et al. Atrial Fibrillation Catheter Ablation vs Medical Therapy and Psychological Distress: a Randomized Clinical Trial. *JAMA*. 2023;330(10):925–933. doi:10.1001/jama.2023.14685
6. Parameswaran R, Al-Kaisey AM, Kalman JM. Catheter ablation for atrial fibrillation: current indications and evolving technologies. *Nat Rev Cardiol*. 2021;18(3):210–225. doi:10.1038/s41569-020-00451-x
7. Gunawardene MA, Willems S. Atrial fibrillation progression and the importance of early treatment for improving clinical outcomes. *Europace*. 2022;24(Suppl 2):ii22–ii28. doi:10.1093/europace/eaab257
8. Newton K, Strasser A, Kayagaki N, Dixit VM. Cell death. *Cell*. 2024;187(2):235–256. doi:10.1016/j.cell.2023.11.044
9. Yuan J, Ofengeim D. A guide to cell death pathways. *Nat Rev Mol Cell Biol*. 2024;25(5):379–395. doi:10.1038/s41580-023-00689-6
10. Dixon SJ, Olzmann JA. The cell biology of ferroptosis. *Nat Rev Mol Cell Biol*. 2024;25(6):424–442. doi:10.1038/s41580-024-00703-5
11. Yamamoto H, Zhang S, Mizushima N. Autophagy genes in biology and disease. *Nat Rev Genet*. 2023;24(6):382–400. doi:10.1038/s41576-022-00562-w
12. Cai K, Jiang H, Zou Y, et al. Programmed death of cardiomyocytes in cardiovascular disease and new therapeutic approaches. *Pharmacol Res*. 2024;206:107281. doi:10.1016/j.phrs.2024.107281
13. Bedoui S, Herold MJ, Strasser A. Emerging connectivity of programmed cell death pathways and its physiological implications. *Nat Rev Mol Cell Biol*. 2020;21(11):678–695. doi:10.1038/s41580-020-0270-8
14. Yu LM, Dong X, Huang T, et al. Inhibition of ferroptosis by icariin treatment attenuates excessive ethanol consumption-induced atrial remodeling and susceptibility to atrial fibrillation, role of SIRT1. *Apoptosis*. 2023;28(3–4):607–626. doi:10.1007/s10495-023-01814-8
15. Zhou JB, Qian LL, Wu D, Wang RX. The Role of Ferroptosis in Atrial Fibrillation: a Promising Future. *Rev Cardiovasc Med*. 2024;25(4):127. doi:10.31083/j.rcm.2504127
16. He L, Liu R, Yue H, et al. Interaction between neutrophil extracellular traps and cardiomyocytes contributes to atrial fibrillation progression. *Signal Transduct Target Ther*. 2023;8(1):279. doi:10.1038/s41392-023-01497-2
17. Lv Y, Du J, Xiong H, et al. Machine learning-based analysis of programmed cell death types and key genes in intervertebral disc degeneration. *Apoptosis*. 2025;30(1–2):250–266. doi:10.1007/s10495-024-02047-z
18. Liu Y, Yang X, Gan J, Chen S, Xiao ZX, Cao Y. CB-Dock2: improved protein-ligand blind docking by integrating cavity detection, docking and homologous template fitting. *Nucleic Acids Res*. 2022;50(W1):W159–W164. doi:10.1093/nar/gkac394
19. Mace LC, Yermalitskaya LV, Yi Y, Yang Z, Morgan AM, Murray KT. Transcriptional remodeling of rapidly stimulated HL-1 atrial myocytes exhibits concordance with human atrial fibrillation. *J Mol Cell Cardiol*. 2009;47(4):485–492. doi:10.1016/j.yjmcc.2009.07.006
20. van Gorp PRR, Trines SA, Pijnappels DA, de Vries AAF. Multicellular In vitro Models of Cardiac Arrhythmias: focus on Atrial Fibrillation. *Front Cardiovasc Med*. 2020;7:43. doi:10.3389/fcvm.2020.00043
21. Shaihov-Teper O, Ram E, Ballan N, et al. Extracellular Vesicles From Epicardial Fat Facilitate Atrial Fibrillation. *Circulation*. 2021;143(25):2475–2493. doi:10.1161/CIRCULATIONAHA.120.052009
22. Xu S, Tao H, Cao W, et al. Ketogenic diets inhibit mitochondrial biogenesis and induce cardiac fibrosis. *Signal Transduct Target Ther*. 2021;6(1):54. doi:10.1038/s41392-020-00411-4
23. Wang F, Gómez-Sintes R, Boya P. Lysosomal membrane permeabilization and cell death. *Traffic*. 2018;19(12):918–931. doi:10.1111/tra.12613
24. Milani M, Pihán P, Hetz C. Calcium signaling in lysosome-dependent cell death. *Cell Calcium*. 2023;113:102751. doi:10.1016/j.ceca.2023.102751
25. Alam S, Afsar SY, Wolter MA, et al. SIP Lyase Deficiency in the Brain Promotes Astroglialosis and NLRP3 Inflammasome Activation via Purinergic Signaling. *Cells*. 2023;12(14). doi:10.3390/cells12141844
26. Yuan F, Wang Z, Sun Y, et al. Sgpl1 deletion elevates SIP levels, contributing to NPR2 inactivity and p21 expression that block germ cell development. *Cell Death Dis*. 2021;12(6):574. doi:10.1038/s41419-021-03848-9
27. Mitroi DN, Karunakaran I, Gräler M, et al. SGPL1 (sphingosine phosphate lyase 1) modulates neuronal autophagy via phosphatidylethanolamine production. *Autophagy*. 2017;13(5):885–899. doi:10.1080/15548627.2017.1291471
28. Xu Y, Zhang Q, Tan L, Xie X, Zhao Y. The characteristics and biological significance of NPC2: mutation and disease. *Mutat Res Rev Mutat Res*. 2019;782:108284. doi:10.1016/j.mrev.2019.108284
29. Alvarez-Valadez K, Sauvat A, Diharce J, et al. Lysosomal damage due to cholesterol accumulation triggers immunogenic cell death. *Autophagy*. 2025;21(5):934–956. doi:10.1080/15548627.2024.2440842
30. Sapaly D, Cheguillaume F, Weill L, et al. Dysregulation of muscle cholesterol transport in amyotrophic lateral sclerosis. *Brain*. 2025;148(3):788–802. doi:10.1093/brain/awae270
31. Pfrieger FW. The Niemann-Pick type diseases - A synopsis of inborn errors in sphingolipid and cholesterol metabolism. *Prog Lipid Res*. 2023;90:101225. doi:10.1016/j.plipres.2023.101225
32. Lee D, Hong JH. Niemann-Pick Disease Type C (NPDC) by Mutation of NPC1 and NPC2: aberrant Lysosomal Cholesterol Trafficking and Oxidative Stress. *Antioxidants*. 2023;12(12):2021. doi:10.3390/antiox12122021
33. Lee MY, Han S, Bang OY, et al. Drug Utilization Pattern of Oral Anticoagulants in Patients with Atrial Fibrillation: a Nationwide Population-Based Study in Korea. *Adv Ther*. 2022;39(7):3112–3130. doi:10.1007/s12325-022-02151-z
34. Boriani G, Vitolo M, Diemberger I, et al. Optimizing indices of atrial fibrillation susceptibility and burden to evaluate atrial fibrillation severity, risk and outcomes. *Cardiovasc Res*. 2021;117(7):1–21. doi:10.1093/cvr/cvab147

35. Yao Y, Yang M, Liu D, Zhao Q. Immune remodeling and atrial fibrillation. *Front Physiol.* 2022;13:927221. doi:10.3389/fphys.2022.927221
36. Hulsmans M, Schloss MJ, Lee IH, et al. Recruited macrophages elicit atrial fibrillation. *Science.* 2023;381(6654):231–239. doi:10.1126/science.abq3061
37. Kany S, Jurgens SJ, Rämö JT, et al. Genetic testing in early-onset atrial fibrillation. *Eur Heart J.* 2024;45(34):3111–3123. doi:10.1093/eurheartj/ehae298
38. Wu D, Deng D, Tang B. Programmed Cell Death in Heart Failure: mechanisms, Impacts, and Therapeutic Prospects. *Rev Cardiovasc Med.* 2025;26(7):38407. doi:10.31083/RCM38407
39. Lisa S, Ha Elizabeth E, Lo James C. Metabolic and Inflammatory Mechanisms Driving Atrial Fibrillation. *Annu Rev Pharmacol Toxicol.* 2025. doi:10.1146/annurev-pharmtox-062124-025403
40. Otsuda T, Aihara K, Takayama T. Lysosomal Stress in Cardiovascular Diseases: therapeutic Potential of Cardiovascular Drugs and Future Directions. *Biomedicines.* 2025;13(5):1053. doi:10.3390/biomedicines13051053
41. Wang S, Wang Y, Qiu K, Zhu J, Wu Y. RCAN1 in cardiovascular diseases: molecular mechanisms and a potential therapeutic target. *Mol Med.* 2020;26(1):118. doi:10.1186/s10020-020-00249-0
42. Jens V, Kim NM, Marcel B, et al. Sphingosine-1-Phosphate Lyase Inhibition Increases Glycolysis in Adult Cardiomyocytes and Restores Glycolytic Flux in Diabetic Cardiomyopathy. *J Cell Mol Med.* 2025;29(21):e70924. doi:10.1111/jcmm.70924
43. Hu Q, Zhang J, Luo X, et al. Intracellular L-PGDS-Derived 15d-PGJ2 Inhibits CaMKII Through Lipoxidation to Alleviate Cardiac Ischemia/Reperfusion Injury. *Circulation.* 2025;152(1):41–57. doi:10.1161/CIRCULATIONAHA.124.070936
44. Li Y, Pereda Serras C, Blumenfeld J, et al. Cell-type-directed network-correcting combination therapy for Alzheimer's disease. *Cell.* 2025. doi:10.1016/j.cell.2025.06.035
45. Kukendrarajah K, Farmaki AE, Lambiase PD, et al. Advancing drug development for atrial fibrillation by prioritising findings from human genetic association studies. *EBioMedicine.* 2024;105:105194. doi:10.1016/j.ebiom.2024.105194

Journal of Inflammation Research

Publish your work in this journal

The Journal of Inflammation Research is an international, peer-reviewed open-access journal that welcomes laboratory and clinical findings on the molecular basis, cell biology and pharmacology of inflammation including original research, reviews, symposium reports, hypothesis formation and commentaries on: acute/chronic inflammation; mediators of inflammation; cellular processes; molecular mechanisms; pharmacology and novel anti-inflammatory drugs; clinical conditions involving inflammation. The manuscript management system is completely online and includes a very quick and fair peer-review system. Visit <http://www.dovepress.com/testimonials.php> to read real quotes from published authors.

Submit your manuscript here: <https://www.dovepress.com/journal-of-inflammation-research-journal>

Dovepress
Taylor & Francis Group